(NASA-CR-199801) THERMALLY INDUCED DAMAGE IN COMPOSITE SPACE STRUCTURE: PREDICTIVE METHODOLOGY AND EXPERIMENTAL CORRELATION (MIT) 25 p

N96-16100

Unclas

G3/24 0085079

NASA-CR-199801

THERMALLY INDUCED DAMAGE IN COMPOSITE SPACE STRUCTURE: PREDICTIVE METHODOLOGY AND EXPERIMENTAL CORRELATION

NAG1-1463
IN-24-CR
6501
p. 25

Cecelia H. Park and Hugh L. McManus

Department of Aeronautics and Astronautics, Massachusetts Institute of Technology, Cambridge, MA 02139, USA

ABSTRACT

A general analysis method is presented to predict matrix cracks in all plies of a composite laminate, and resulting degraded laminate properties, as functions of temperature or thermal cycles. A shear lag solution of the stresses in the vicinity of cracks and a fracture mechanics crack formation criteria are used to predict cracks. Damage is modeled incrementally, which allows the inclusion of the effects of temperature dependent material properties and softening of the laminate due to previous cracking. The analysis is incorporated into an easy-to-use computer program. The analysis is correlated with experimentally measured crack densities in a variety of laminates exposed to monotonically decreasing temperatures. Crack densities are measured at the edges of specimens by microscopic inspection, and throughout the specimen volumes by X-ray and sanding down of the edges. Correlation between the analytical results and the crack densities in the interiors of the specimens was quite good. Crack densities measured at specimen edges did not agree with internal crack densities (or analyses) in some cases. A free-edge stress analysis clarified the reasons for these discrepancies.

BACKGROUND

Advanced composite materials are commonly used in dimensionally critical space structures. However, the wide swings in temperature that occur as an orbiting vehicle moves in and out of the earth's shadow can cause cracks in these materials. The cracks, dubbed matrix cracks or

microcracks, are found in the individual plies, parallel to the fibers. They are caused by coefficient of thermal expansion (CTE) mismatch between plies of different orientations. Microcracks alter the thermal and mechanical properties of the laminate, unfavorably affecting dimensional stability.

Microcracking due to mechanical loading and mechanical fatigue has been extensively studied. The present work draws on this rich background, but it will not be reviewed here, except to acknowledge the work of Laws and Dvorak[1]. The crack formation model used here is based on this work. A more extensive review can be found in Reference 2.

Many mechanical loading studies have included the effects of residual thermal stresses, but only a limited amount of work has been done to directly address the cracking of thermally loaded composites. Adams[3] used Classical Laminated Plate Theory (CLPT) and *in situ* transverse strength to predict the onset of microcracking. The ply discount method was used by Bowles[4] to predict reduction of properties with little success. These analyses emphasize damage at the ply level. Micromechanics methods approach the problem at a different scale to study fiber and matrix interactions. For example, Bowles[5] derived thermally induced stresses using a finite element analysis. He then predicted fiber-matrix debonding initiation and location by comparing the maximum radial stress at the interface to the interfacial bond strength.

Most of the research dedicated to the thermal loading problem has been experimental. Knouff[6] found fiber type and properties had an effect on microcracking under thermal cycling. Numerous experiments were conducted by Tompkins et al.[7-10] to measure properties such as CTE, stiffness, strain and crack density after thermal cycling. Manders and Maas[11] tested laminates made from very thin plies to see if cracking and property degradation could be prevented. Bowles and Shen[12] tested fabric for the same purposes.

McManus et al.[13] developed an analytical method for thermally loaded laminates. Crack density in one ply group, and reduced laminate properties due to these cracks, were predicted as functions of monotonically decreasing temperature. The effects of thermal cycling were included in the analysis using a material degradation fatigue model. Experimentally, specimens were monotonically cooled and inspected at the edges for cracks. Thermal cycling tests were

also performed. The analyses correlated very well with the experiments. However, the method is severely limited in its practical use by the ability to predict crack density in one ply group.

STATEMENT OF PROBLEM

Given laminate geometry, layup, material property information and thermal loading history, crack density and degraded laminate properties are predicted. The method can analyze all plies in an arbitrary layup under monotonically increasing or cyclic thermal loading. Progressive material softening effects and temperature dependent material properties are included. In this work, this capability is pursued by 1) developing a generalized analytical tool, 2) correlating the analysis with experiments, and 3) studying the validity of the assumptions underlying the analytical method.

ANALYTICAL MODEL

Geometry. Figure 1 shows a laminate aligned with a global coordinate system xyz. We will determine the properties of this laminate in the global x-direction. The laminate is made up of unidirectional plies. Stacked plies with the same ply angle are assumed to act as a single thick ply, referred to as a ply group. Cracks are assumed to span the ply group thickness and propagate parallel to the fibers through the width of the composite laminate. Figure 1 shows cracks of this type in a laminate with three ply groups. A local coordinate system $x'y'z'$ is defined for each crack. The y' axis is aligned with the crack, parallel to the fiber direction of the ply group, the x' axis is aligned with the transverse direction of the ply group, and the origin is at the center of the crack.

Crack formation. To predict cracking in any one ply group, the laminate is modeled as being made up of two components: the cracking ply group and the rest of the laminate, which is smeared. Figure 2 shows a cross section of the laminate, aligned with the local coordinate system of a hypothetical new crack which is postulated between two existing cracks. The laminate is subjected to a thermal load ΔT which is the difference between the current temperature and some stress free temperature, usually taken to be the cure temperature.

If the new crack forms, some of the strain energy stored in the laminate due to the thermal load will be released. A one-dimensional shear lag model is used to estimate this energy. Laminate and cracking ply group properties are calculated in the x'-direction. The stress and displacement fields are found with and without the hypothetical new crack, and the strain energy in each case is then calculated. The difference between these strain energies is the energy that would be released by the appearance of the new crack. This is expressed, per unit area of new crack surface, as the energy release rate G_I. If G_I is greater than the critical stain energy release rate of the material G_{Ic}, the hypothetical crack will in fact form. This basic energy criteria is expressed as a function of applied thermal loading. The development[2] is lengthy, and will not be presented here. The final expression is:

$$G_I = \frac{a_r a_c E_r E_c (\alpha_c - \alpha_r)^2 \Delta T^2}{2\xi(a_r E_r + a_c E_c)} \left[2\tanh\left(\frac{\xi h}{a_c}\right) - \tanh\left(\frac{2\xi h}{a_c}\right) \right] \qquad (1)$$

The subscripts c and r represent properties of the cracking ply group and the rest of the laminate, respectively. Thus, α_c is the CTE of the cracking ply group, α_r is the smeared CTE of the rest of the laminate, E_c is the uncracked stiffness of the cracking ply group, and E_r is the smeared stiffness of the remainder of the laminate, all in the x' direction. The thickness of the cracking ply group is a_c, and a_r is the thickness of the rest of the laminate. The geometric fitting factor ξ is fixed at a value used in prior studies[13].

Assuming an existing uniform crack spacing $2h$, a corresponding ΔT is found which satisfies Eq. 1 with G_I set equal to G_{Ic}. At any thermal load greater than this ΔT, new cracks will form midway between the existing cracks. Therefore, the minimum possible crack density at this ΔT is defined as ρ, where $\rho = 1/(2h)$. Note that Eq. 1 can be solved explicitly for ΔT given h, but if h (or ρ) for a given ΔT is required, it must be solved for graphically or numerically.

Laminate property constants. The constants used in the above analysis are calculated by CLPT[14]. First, appropriate material properties are obtained as functions of temperature or cycle number. For each ply i of thickness t_i, these are E_{li} (longitudinal stiffness), E_{ti} (transverse stiffness), ν_i (major Poisson's ratio), G_i (shear stiffness) α_{li} (longitudinal CTE) and α_{ti}

(transverse CTE). The fibers of each ply are aligned at an angle θ_i to the global coordinate system.

The crack formation analysis is carried out for each ply group in turn. The ply group considered is dubbed the cracking ply group. The subscript *c* denotes this group, hence it has orientation θ_c. The analysis is carried out in the local coordinate system *x'y'z'* defined above. In this coordinate system, the ply angles are defined:

$$\theta_i' = \theta_i + 90° - \theta_c \tag{2}$$

The necessary laminate properties for computing crack density and property degradation can be calculated using familiar CLPT relations. The laminate stiffness in the x'y'z' coordinate system is

$$\mathbf{A} = \sum_{i=1}^{n} \overline{\mathbf{Q}}_i t_i \tag{3}$$

The rotated reduced ply stiffnesses in the x'y'z' system are

$$\overline{\mathbf{Q}}_i = \mathbf{T}_i^{-1} \mathbf{Q}_i \mathbf{T}_i^{-\mathrm{T}} \tag{4}$$

where

$$\mathbf{T}_i = \begin{bmatrix} \cos^2\theta_i' & \sin^2\theta_i' & 2\sin\theta_i'\cos\theta_i' \\ \sin^2\theta_i' & \cos^2\theta_i' & -2\sin\theta_i'\cos\theta_i' \\ -\sin\theta_i'\cos\theta_i' & \sin\theta_i'\cos\theta_i' & \cos^2\theta_i' - \sin^2\theta_i' \end{bmatrix} \tag{5}$$

and

$$\mathbf{Q}_i = \begin{bmatrix} Q_{11(i)} & Q_{12(i)} & 0 \\ Q_{12(i)} & Q_{22(i)} & 0 \\ 0 & 0 & Q_{66(i)} \end{bmatrix} \tag{6}$$

and the reduced ply stiffnesses are

$$\begin{aligned} Q_{11(i)} &= \frac{E_{li}}{D_i} & Q_{12(i)} &= \kappa_i \frac{\nu_i E_{ti}}{D_i} \\ Q_{22(i)} &= \kappa_i \frac{E_{ti}}{D_i} & Q_{66(i)} &= \kappa_i \frac{G_i}{D_i} \end{aligned} \qquad D_i = 1 - \nu_i^2 \frac{E_{ti}}{E_{li}} \tag{7}$$

Here κ_i is a knockdown factor which accounts for the effects of pre-existing cracks. Initially it

has the value 1. The CTE's of each ply are

$$\boldsymbol{\alpha}_i = \begin{Bmatrix} \alpha_{li} \\ \alpha_{ti} \\ 0 \end{Bmatrix} \tag{8}$$

In the x'y'z' system the ply CTE's are

$$\bar{\boldsymbol{\alpha}}_i = \mathbf{T}_i^{\mathrm{T}} \boldsymbol{\alpha}_i \tag{9}$$

The laminate constants required in Eq.1 are now calculated. The total laminant thickness a_o, is

$$a_o = \sum_{i=1}^{n} t_i \tag{10}$$

The necessary constants for the cracking ply group are

$$E_c = \frac{E_{tc}}{D_c} \qquad \alpha_c = \alpha_{tc} \qquad a_c = t_c \tag{11}$$

and the smeared properties of the rest of the laminate are

$$E_r = \frac{A_{11} - E_c a_c}{a_r} \qquad \alpha_r = \alpha_1^r \qquad a_r = a_o - a_c \tag{12}$$

The smeared CTE of the remaining plies α_1^r is the first element of the vector of CTEs which are calculated

$$\boldsymbol{\alpha}^r = [\mathbf{A} - \bar{\mathbf{Q}}_c t_c]^{-1} \left(\sum_{i=1}^{n} \bar{\mathbf{Q}}_i \bar{\boldsymbol{\alpha}}_i t_i - \bar{\mathbf{Q}}_c \bar{\boldsymbol{\alpha}}_c t_c \right) \tag{13}$$

Equation 1 can now be solved to predict the crack density in the cracking ply group ρ_c. The knockdown factor for this group is also recalculated, using the relation developed in Reference 13:

$$\kappa_c = E_c a_c \left(1 - \frac{\rho_c a_c}{2\xi} \tanh \frac{2\xi}{\rho_c a_c} \right) \Bigg/ \left(E_r a_r + E_c a_c \frac{\rho_c a_c}{2\xi} \tanh \frac{2\xi}{\rho_c a_c} \right) \tag{14}$$

After all the ply groups have been analyzed in this manner, the degraded effective laminate properties in the global x direction (stiffness E^{eff} and CTE α^{eff}) are calculated:

$$E^{eff} = \frac{1}{A_{11}^{inv} a_o} \qquad \mathbf{A}^{inv} = \mathbf{A}^{-1} \qquad \alpha^{eff} = \alpha_1^a \tag{15}$$

where α_1^e is the first element of

$$\alpha^e = \mathbf{A}^{-1} \sum_{i=1}^{n} \overline{\mathbf{Q}}_i \overline{\alpha}_i t_i \tag{16}$$

and $\mathbf{A}$, $\overline{\mathbf{Q}}$ and $\overline{\alpha}$ are calculated from Eqs. 3-9 above with $\theta_i' = \theta_i$. Note no bending is incorporated into the analysis, so it is only strictly valid for symmetric laminates.

Progressive Damage. The material properties depend on temperature and number of temperature cycles, and the stiffness coefficient E_r used to calculate cracking is dependent on existing crack densities through the knockdown factors. An incremental progressive damage solution is used to account for this coupling. Figure 3 is a flow chart of the algorithm used for a monotonically decreasing temperature case. The analysis starts at the stress free temperature and is incrementally decreased. At each new temperature, the material properties are computed. The crack density in each ply group is then calculated. Equation 1 is solved for h using a bisection iteration numerical method. This procedure is repeated for every ply at this temperature. After computing the crack density for every ply group, both the overall laminate properties and the ply knock-down factors are recalculated to reflect all the damage at this temperature. These steps are iterated to calculate crack density and laminate properties at progressively lower temperatures. A similar progressive damage algorithm is used for thermal cycling.

Edge Effects. The analytical procedure developed predicts stresses in each ply of a laminate using the assumptions of CLPT. However, at the free edge of a laminate, the assumptions of CLPT are no longer valid. Given that most experimental results involve observation of microcracks at specimen edges, the free-edge stress state is clearly important. The analysis of Bhat is used to analytically explore the three dimensional free-edge stress state. A modification of the computer code by Bhat computes the in-plane stress distribution in each ply group near a free edge parallel to the global x direction. This analysis is used for comparison to experimental results, but it is not incorporated into the crack prediction calculations. It will be fully described in a later publication.

COMPUTER PROGRAM

The computer code CRACKOMATIC II takes material properties, laminate geometries, and thermal loading history and predicts crack density and corresponding degraded laminate properties. The two types of calculations are 1) tabulation of crack density and degraded material properties as functions of monotonically decreasing temperature and 2) tabulation of crack density and degraded material properties as functions of thermal cycles. The resulting output is a table with columns listing thermal load (ΔT or N), corresponding crack density of any selected plies, and corresponding reduced laminate properties. These can be used to generate plots of cracking and changing laminate properties as the laminate is thermally cycled or progressively cooled.

The program output reports crack densities as they could be observed on the edge of a specimen. This requires that the calculated results, which are expressed in ply coordinates, be adjusted to account for a geometric effect. Figure 4 illustrates this effect. The figure shows a laminate with cracks in the 45° and 90° direction. The crack spacing (h) is the same, but due to the geometry of the laminate, the edge crack count is higher in the 90° (9 cracks) than in the 45° ply (6 cracks). The reported crack density, ρ_c^{edge}, is the calculated density, ρ_c, multiplied by a geometric factor:

$$\rho_c^{edge} = \rho_c \sin(\theta_c) \tag{10}$$

The CRACKOMATIC II program is available by request from the authors.

EXPERIMENTS

Experiments were conducted to correlate with analytical predictions and to check the assumptions on which the analysis was based. P75/934 and P75/ERL1962 graphite/epoxy laminates listed in Table 1 were fabricated at NASA Langley Research Center using 0.127 mm (0.005") thick plies and vendor recommended cure procedures. Panels 30.5 cm × 30.5 cm (12" × 12") were cut into 7.6 cm × 1.2 cm (3.0" × 0.5") specimens. All the specimens were dried to a constant weight to eliminate absorption effects.

Specimens were monotonically cooled to progressively lower temperatures in a thermal

environmental chamber. Starting at room temperature, the specimens were cooled to target temperatures as low as -157°C (-250°F) at a rate of 14°C/min. The cooling and heating rates were low enough to avoid significant thermal gradients in the specimens. Specimens were soaked at the target temperature for 5 minutes and returned to room temperature. The edges of the specimens were then inspected for cracks under an optical microscope at 200× magnification. An observed crack extending more than half the thickness of a ply or ply group was counted as a crack. The crack configuration throughout the volume of the laminate was determined using dye-penetrant enhanced X-radiography and a series of edge inspections done after sanding down the edges of the specimens. Control experiments were performed to assure that the sanding procedure did not create additional cracks; details are found in Reference 2.

RESULTS

The experimental results were compared with analytical predictions made using the material properties in Table 2. The material properties were assumed to be temperature independent. Selected results from Reference 2 are presented here. Crack densities are plotted as functions of decreasing temperature. Experimental results shown are average values with one standard deviation error bars. Edge inspection data is collected from two or more specimens, while interior data is collected from eight or more points in a single specimen by sanding down the specimen edges.

Thick Ply Groups. The $[0_2/45_2/90_2/-45_2]_s$ specimens were produced specifically because they have thick ply groups (two or more plies oriented in the same direction stacked together) that produce large cracks that can be easily observed. The crack distributions measured by edge inspection and X-ray are identical, and the X-ray pictures show the cracks continued through the laminate as shown in Figure 1. The analytical predictions of crack densities at low temperatures (-157°C) match the data very well (Figure 5), but the development of the cracks with decreasing temperature is overpredicted in the central -45_4 ply group, and underpredicted in the 90_2 groups. These results contrast with the good predictions of cracking in the 90_4 ply group of a $[0_2/90_2]_s$ laminate achieved by McManus et al.[13]. Analysis of both the 45_2 ply

groups in this laminate, and the -45_2 ply groups in the $[0/45/90/-45]_s$ laminate, show good agreement with the trends seen in the data, but overpredict the number of cracks [2].

Single Plies. Single plies do not crack in the simple way shown in Figure 1. The cracks do go from the top to the bottom of each ply (so cross-sections such as shown in Figure 2 have the expected appearance), but do not go straight through the width of the specimen. Without continuous cracks to follow, the X-ray dye cannot penetrate into the specimen, so no cracks are visible in these plies in the X-ray photos. Sanding down specimen edges reveals large variations in crack densities within each specimen. The 30° plies in the $[0/\pm30]_s$ laminates are predicted to remain uncracked during testing. A few cracks are observed at specimen edges, but none in the interior of specimens. Conversely, there are many more cracks in the single 45° plies of $[0/45/90/-45]_s$ laminates away from the edges than near edges. The correlation between the analytical predictions and the crack densities measured at the specimen free edges is poor, while the correlation between the analytical prediction and the average internal crack density is quite good (Figure 6). Cracks are observed at the edges of 90° plies at higher temperatures than predicted (Figure 7), while the internal crack density correlation is inconclusive.

Property Changes. The change of laminate properties due to cracking was studied analytically. The laminate stiffness and CTE changes in a $[0/45/90/-45]_s$ laminate due to predicted microcracking are shown in Figures 8 and 9 respectively. In both cases, the effect of cracking in the central -45_2 ply group is seen first, followed by the effects of cracking in the 45° and 90° plies. Figure 8 shows normalized laminate longitudinal stiffness versus decreasing temperature and illustrates the small change in stiffness seen in all laminates considered. Figure 9 shows the CTE is greatly affected by thermal loading and cracking. The values change about 300% in the 25°C to -157°C temperature range. The figures do not show temperature dependent material properties; the results reflect permanent property changes due to cracking damage.

Edge effects. The free edge stress solution is shown in Figure 10 for the $[0/45/90/-45]_s$ laminate. The stress transverse to the fiber direction in each ply group of a thermally loaded $[0/45/90/-45]_s$ laminate is shown through the first 2mm from the free edge. The stresses reach expected (CLPT) values by 1mm into the laminate. The transverse stress in the 45° ply groups

drops to zero near the free edge.

DISCUSSION AND CONCLUSIONS

A method useful for predicting thermally induced cracking in composite laminates, and its effects on laminate properties, has been developed. In contrast with previous work, which concentrated on single transverse ply groups in simple laminates, cracking is predicted in all plies in an arbitrary laminate. Experimental correlations show the method works well for predicting volume average crack densities created when laminates are exposed to low temperatures.

The method does not correlate well with edge crack counts in some cases. Two effects, not accounted for by the assumptions used to develop the analysis, explain these descrepencies: the configuration of the cracks, and the effects of the specimen free edges. Cracks in groups of two or more 0.128 mm plies with the same orientation behave in the assumed way, with cracks continuous through the width of the laminate. Single plies do not crack in this fashion. Cracks are short, and crack density varies widely through the width of the laminate. Near edges, angle plies (such as 45° plies) show much lower levels of cracking than in the interior. This is due to the low transverse stresses in these plies near free edges. Conversely, 90° plies show slightly more cracks near edges. The reason for this is less clear, but it has been noted that these plies are sensitive to handling[2] and the exact condition of the edge during loading [2,15].

This work shows that edge crack counts, which have been accepted as a useful metric of damage, are not necessarily good indicators of the internal state of the laminate. This problem does not appear in thick, multiply groups, typical of the specimens used in many prior studies, but it is acute for thin individual plies typical of spacecraft structure. For these structures, both new screening test techniques (to replace edge crack counting) and improved analytical techniques (to incorporate the effects of free edges and to account for the non-ideal nature of cracks in these plies) are needed.

ACKNOWLEDGMENT

This work was supported by NASA Grant NAG-1-1463, supervised by Steve Tompkins.

REFERENCES

1. N. Laws. and G. Dvorak, Progressive Transverse Cracking in Composite Laminates, *Journal of Composite Materials*, 22 (1988) pp. 900-916.
2. C. H. S. Park, Analysis of Thermally Induced Damage in Composite Space Structures, *Master of Science Thesis*, Massachusetts Institute of Technology, 1994.
3. D. Adams, D. Bowles, and C. Herakovich, Thermally Induced Transverse Cracking in Graphite/Epoxy Cross-Ply Laminates, *Journal of Reinforced Plastics and Composites*, 5 (1986) pp. 152-169.
4. D. Bowles, Effect of Microcracks on the Thermal Expansion of Composite Laminates, *Journal of Composite Materials*, 18 (1984) pp. 173-187.
5. D. Bowles, and O. Griffin, Micromechanics Analysis of Space Simulated Thermal Stresses in Composites. Part I: Theory and Unidirectional Laminates and Part II: Multidirectional Laminates and Failure Predictions, *Journal of Reinforced Plastics and Composites*, 10 (1991) pp. 505-539.
6. B. Knouff, S. Tompkins, and N. Jayaraman, The Effect of Graphite Fiber Properties on Microcracking Due to Thermal Cycling of Epoxy-Cynate Matrix Laminates, *ASTM Fifth Symposium on Composite Materials: Fatigue and Fracture*, Atlanta, GA (1993) pp. 2-27.
7. S. Tompkins, and S. Williams, Effects of Thermal Cycling on Mechanical Properties of Graphite Polyimide, *Journal of Spacecraft and Rockets*, 21 (1984) pp. 274-279.
8. S. Tompkins, D. Bowles, W. Slemp, and A. Teichman, Response of Composite Materials to the Space Station Orbit Environment, *AIAA/NASA Space Station Symposium*, Williamsburg, VA (1988).
9. S.Tompkins, Effects of Thermal Cycling on Composite Materials for Space Structures, *NASA/SDIO Space Environmental Effects on Materials Workshop*, (1989) pp. 447-470.
10. S. Tompkins, J. Funk, D. Bowles, T. Towell, and J. Connell, Composite Materials for Precision Space Reflector Panels, *SPIE International Symposium and Exhibition on Optical Engineering and Photonics*, Orlando, FL (1992).
11. P. Manders and D. Maas, Thin Carbon Fiber Prepregs for Dimensionally Critical Structures, *SPIE Advances in Optical Structure Systems*, Orlando, FL (1990) pp. 536-545.
12. D. Bowles and J. Shen, Thermal Cycling Effects on the Dimensional Stability of P75 and P75-T300

(Fabric) Hybrid Graphite/Epoxy Laminates, *33rd International SAMPE Symposium and Exhibition*, Anaheim, CA (1988).

13. H. McManus, D. Bowles, and S. Tompkins, Prediction of Thermally Induced Matrix Cracking, *Proceedings of the American Society of Composites*, Cleveland, OH, **8** (1993).

14. R. Jones, Mechanics of Composite Materials, Hemisphere Publishing, 1975.

15. A. Kitano, K. Yoshioka, K. Noguchi, and J. Matsui, Edge Finishing Effects on Transverse Cracking of Cross-Ply CFRP Laminates, *Ninth International Conference on Composite Materials*, Madrid, Spain, **5** (1993) pp. 169-176.

Table 1. Laminates Tested

Layup	Material	Total Specimens
$[0_2/90_2]_s$	P75/934	3
$[0/90/0/90]_s$	P75/934	4
$[0_2/\pm30]_s$	P75/934	3
$[0/45/90/-45]_s$	P75/934	6
$[0/90/\pm45]_s$	P75/934	4
$[0/\pm45/90]_s$	P75/934	4
$[0_2/45_2/90_2/-45_2]_s$	P75/ERL1962	3

Table 2. Material Properties

Property	P75/934	P75/ERL1962
E_l (GPa)	236	236
E_t (GPa)	6.2	6.6
ν	0.29	0.29
G (GPa)	4.8	4.8
G_{Ic} (J/m2)	40.0	104.0
α_l (με/°C)	-1.22	-0.95
α_t (με/°C)	28.8	39.6
ξ	0.65	0.65

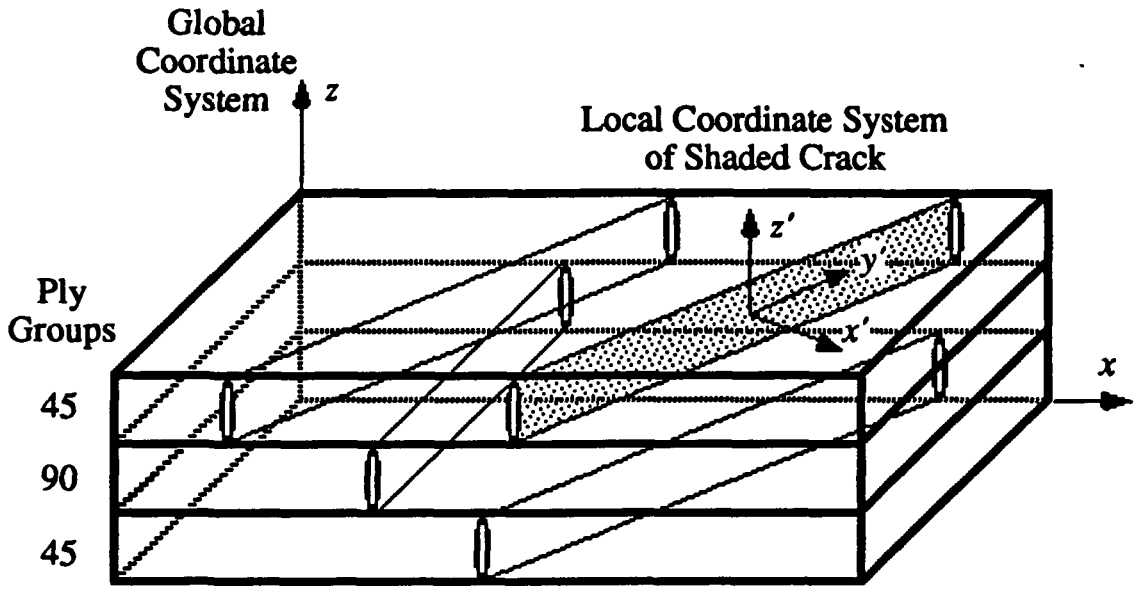

Figure 1. Laminate geometry

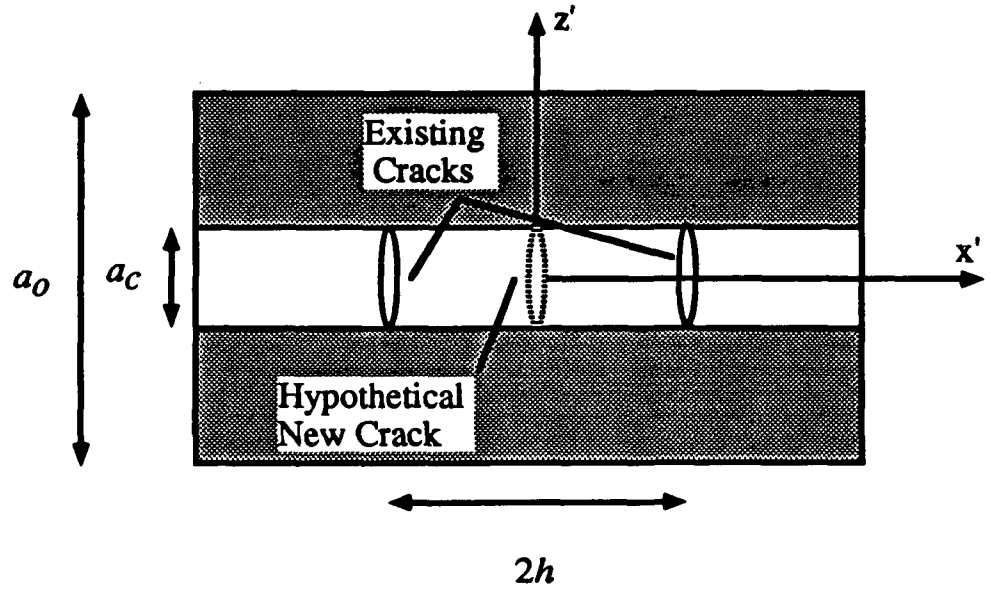

Figure 2. Geometry used in crack calculations

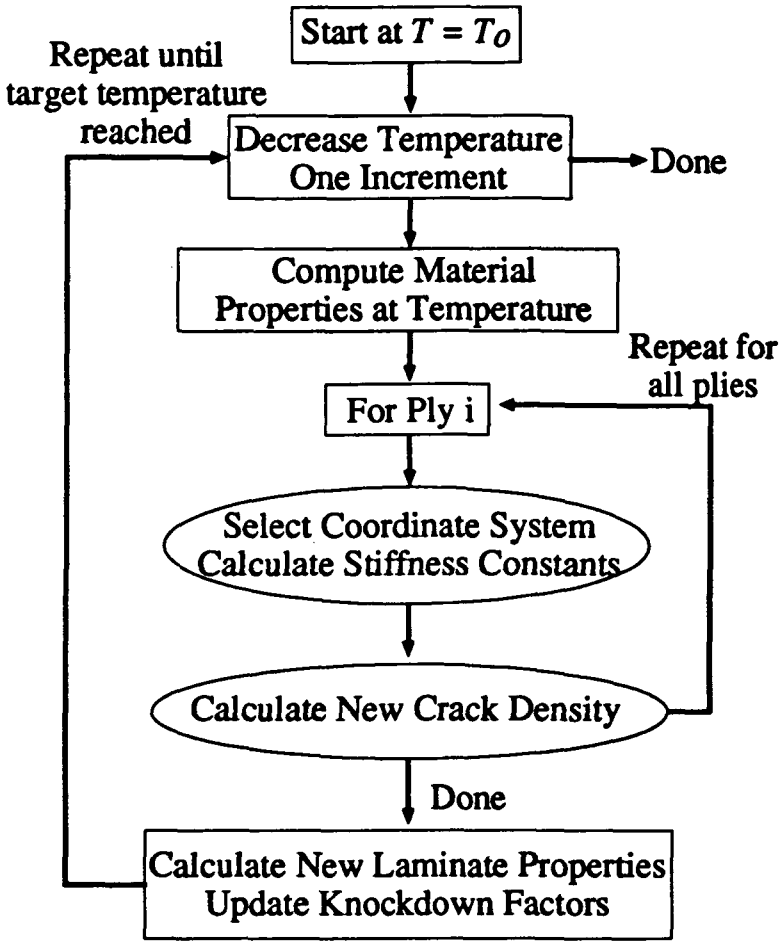

Figure 3. Algorithm flowchart

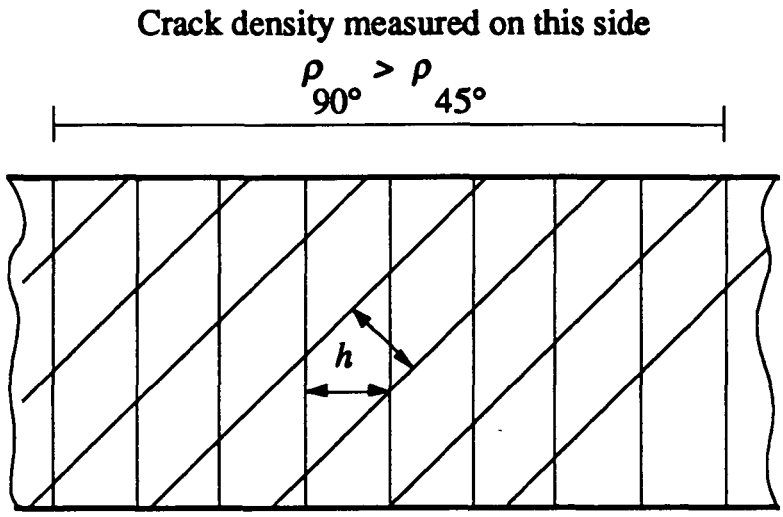

Figure 4. Apparent crack densities

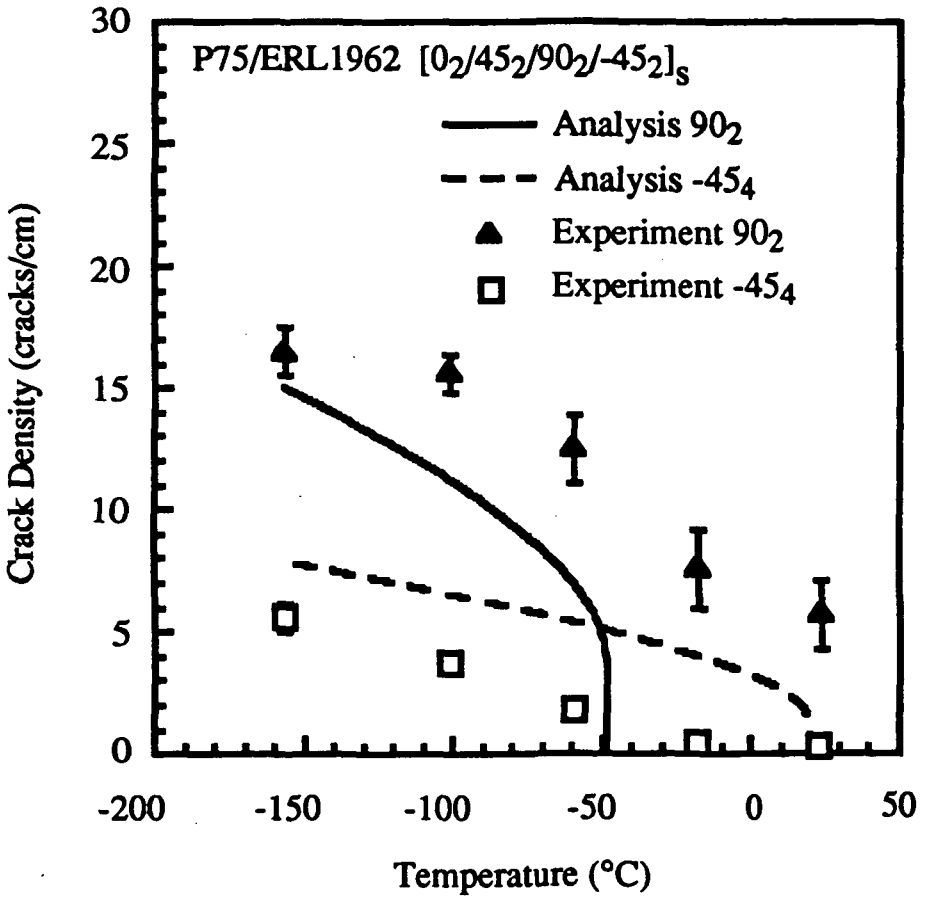

Figure 5. Cracking in two-ply ply groups

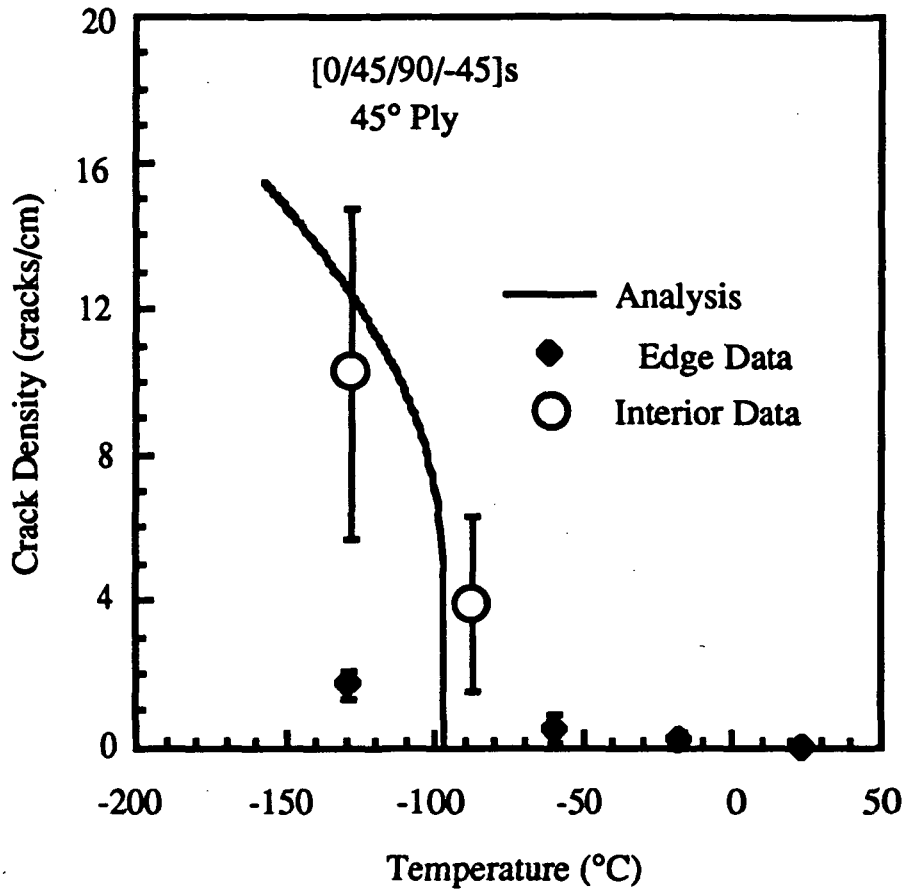

Figure 6. Cracking of thin 45° plies

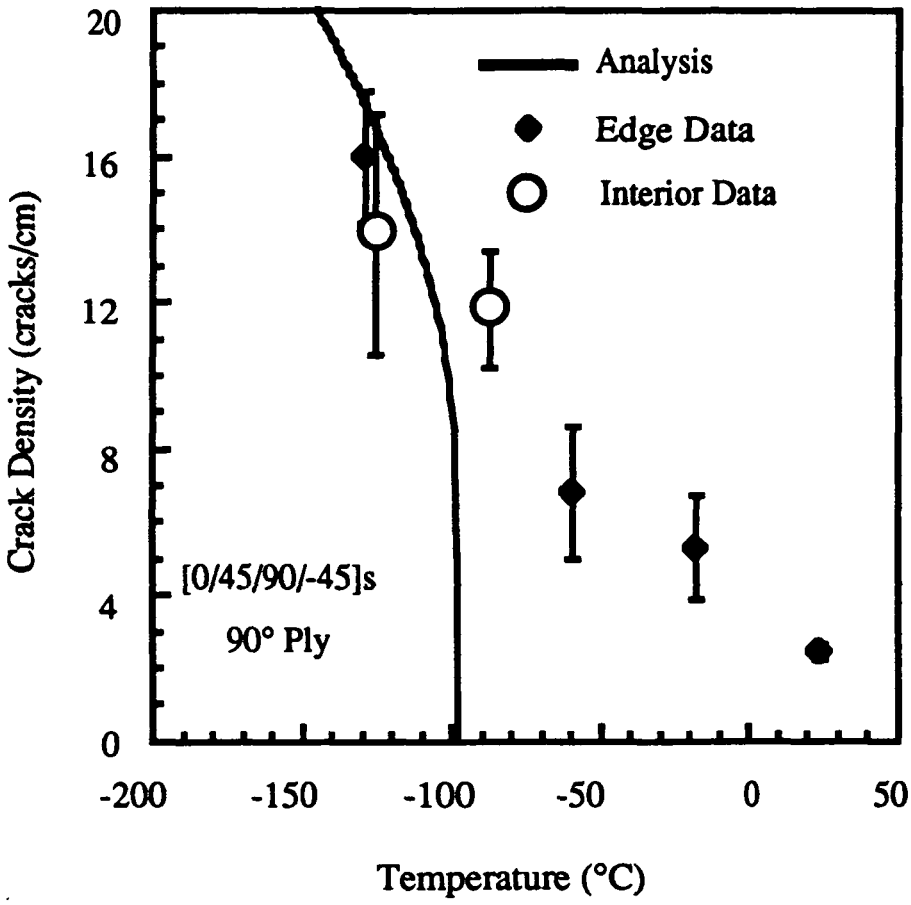

Figure 7. Cracking in thin 90° plies

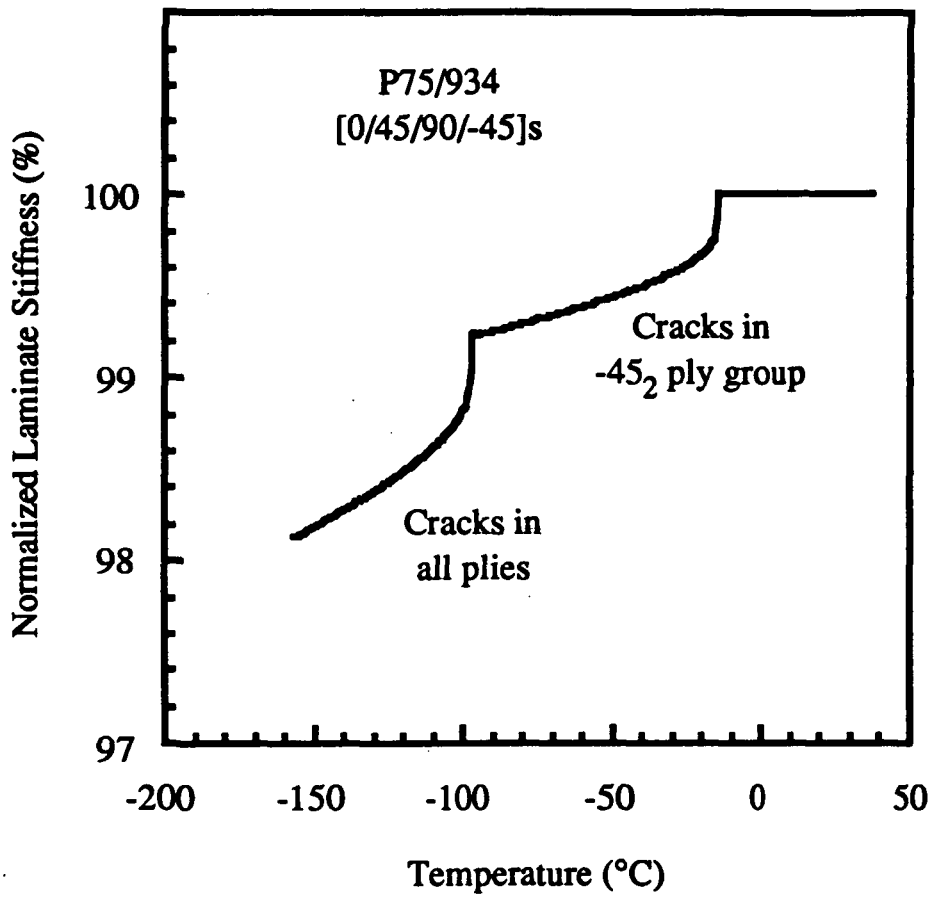

Figure 8. Effect of cracking on laminate longitudinal stiffness

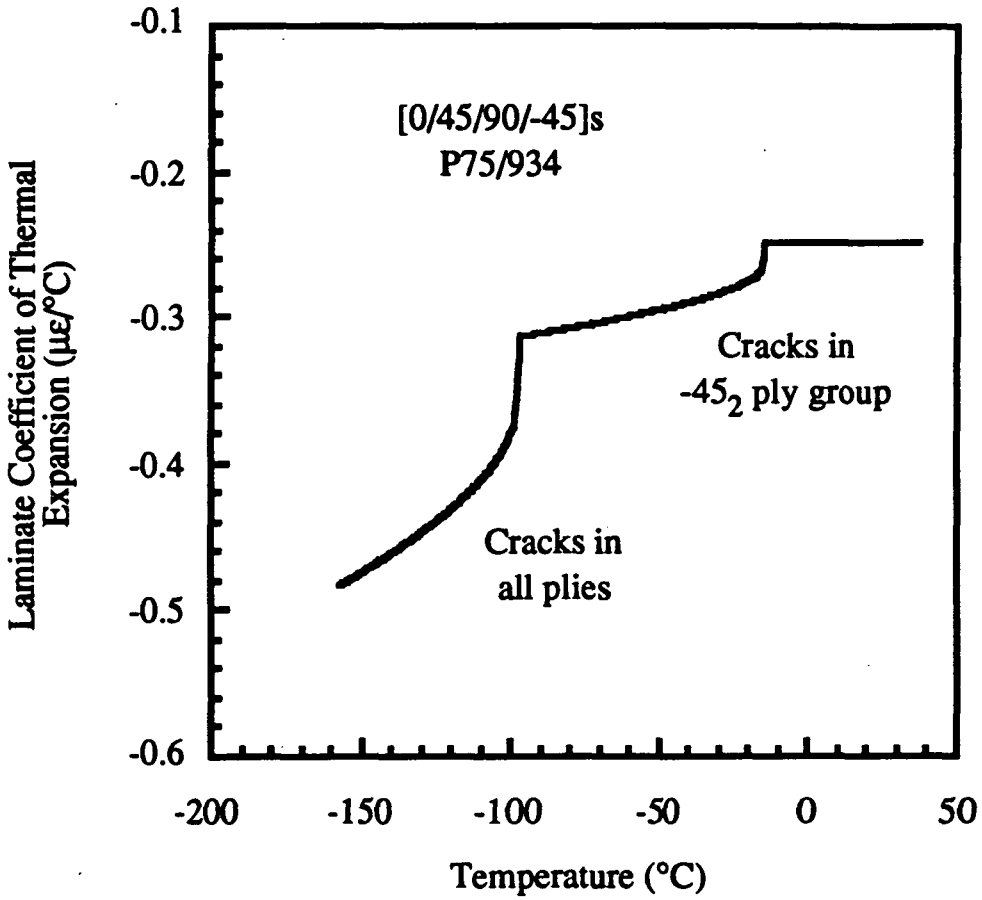

Figure 9. Effect of cracking on laminate longitudinal CTE

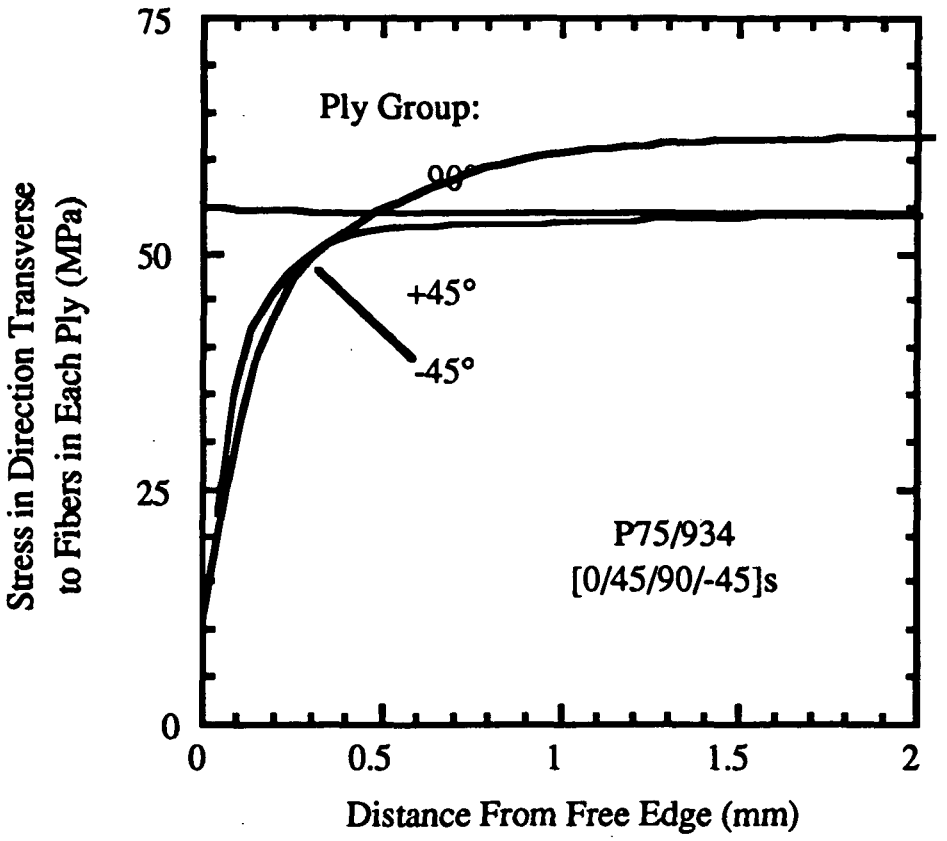

Figure 10. Stresses due to thermal loading near the free edge